



## OPTIMIZATION OF ADSORPTION OF CONGO RED DYE FROM AQUEOUS SOLUTION WITH ACTIVATED CARBON FROM CASTOR SEED SHELL USING CENTRAL COMPOSITE DESIGN

\*H. I. Ohikere, Z. I. Yashim, N. C. Nwokem

Department of Chemistry, Ahmadu Bello University, Zaria-Nigeria.

\*Corresponding authors' email: [hussyohis@gmail.com](mailto:hussyohis@gmail.com)

### ABSTRACT

The present research highlighted the efficacy of activated carbon from castor seed (ACCS) for the removal of Congo red dye from aqueous solution through batch study. Central-Composite Design (CCD) by response surface methodology was used to optimize the adsorption process. Based on CCD design, the quadratic models were developed co-relating the adsorption variables to the removal efficiency. Analysis of variance (ANOVA) was incorporated to judge the adequacy of the model. Fourier Transform Infrared (FTIR) analysis was carried out on ACCS to reveal the functional groups which aided the adsorption of Congo red dye. The model predicted the optimized conditions as follows: initial concentration (100.0 mg/L), adsorption dose (1.2 g), contact time (45.0 mins) and pH (4.0) which resulted to a 99.97% removal efficiency of Congo red dye. Therefore, the present results demonstrate that ACCS is a low-cost alternative for the removal of Congo red dye from aqueous solution.

**Keywords:** Castor seed, adsorption, Congo red dye, Activated carbon

### INTRODUCTION

Water is a very essential requirement in our daily life activities but it is being contaminated by disposal of domestic, municipal and industrial wastes. Industrial development has its attendant consequences on the natural environment most especially on the land natural water bodies. Obvious of these are the textile industries which make heavy use of dyes to color its final products. Synthetic dyestuffs and colors are frequently used in textile, paper, printing industries and dye houses (Garba *et al.*, 2015; Garba *et al.*, 2016; Rápó and Tonk, 2021). The discharge of effluents from these applications is one of the potential sources of environmental contamination and pollution as it is reported that there are over 100,000 commercially available dyes with a production of over  $7 \times 10^5$  metric tons per year. The growth of textile industry in Nigeria contributes a lot of industrial wastewater generated in the country (Garba *et al.*, 2015; Garba *et al.*, 2016; Alsas *et al.*, 2022). Dyes and pigments have been utilized for coloring in the textile industry for many years (Kooh *et al.*, 2016). Several types of textile dyes are available for use with various types of textile materials. Textile wastewater containing dyes are normally discharged into large water bodies (Alsas *et al.*, 2022) and as a result damages the aesthetic nature of water, reduces light penetration through the water surface, and also the photosynthetic activity of aquatic organisms. It also contains toxic and potential carcinogenic substances (Garba *et al.*, 2016; Garba *et al.*, 2021). Therefore, to avoid these hazardous effects, textile wastewater must be adequately treated before they can be discharged into receiving water bodies. There are several applied treatment methods for textile effluents, involving biological, physical or chemical methods and also, combinations of these methods (Rápó and Tonk, 2021)

The consequences of dyes in water bodies are huge. Malik and co-authors reported that 1.0 mg/l dye present in drinking water can significantly affect the color and make the water unhealthy for human consumption (Malik *et al.* 2020; Rápó and Tonk, 2021). In addition, dyes are known to reduce the performance of the aquatic plants and animals because of the reduction in sunlight transmission due to the interference of the dye particles in the water.

A significant number of methods have been harnessed over the years to remove harmful metals and other substances from wastewater; such methods include chemical precipitation, chemical oxidation-reduction, ultrafiltration, reverse osmosis, solvent extraction, ion-exchange, electro dialysis, electrochemical coagulation and evaporation (Alsas *et al.*, 2022). However, these methods have several disadvantages due high operational cost and generation of residual metal sludge after treatment (Alsas *et al.*, 2022). These disadvantages triggered the demand for more economical and efficient methods of wastewater treatment, hence, the development of other separation techniques including adsorption (Adetokun *et al.*, 2019; Afidah and Garba, 2016; Garba *et al.*, 2021; Labaran *et al.*, 2019; Surip *et al.*, 2020; Tan *et al.*, 2020; Xiao *et al.*, 2020; Xiao *et al.*, 2021). Adsorption is a process of using adsorbents for reducing domestic and industrial or tannery effluents (Lofrano *et al.*, 2012)

In the present research work, activated carbon from Castor Seed (ACCS) as adsorbent to remove Congo red dye from aqueous solution was studied.

The idea of optimization relates to maximizing adsorption parameters such as initial concentration, adsorption dose, contact time and pH. The optimization process allows for the comparison of the different choices for determining which might be best (Malik *et al.*, 2020).

Adsorption is a physical-chemical treatment of wastewater in which the dissolved molecule is attached to an adsorbent surface by means of physical and chemical properties. Depending on the nature of the adsorbent and the origin of the dyes, different interactions may be performed, such as electrostatic interaction and Van der Waals forces (Postai *et al.*, 2016). Adsorption as a dye removal method is gaining increasing attention due to its potential efficiency, low energy consumption, high selectivity at molecular level, easy operation, and ability to separate various chemical compounds (Akpomie *et al.*, 2015).

### MATERIALS AND METHODS

#### Sample Collection and Preparation

The castor seed shell was collected from Samaru, Sabon Gari Local Government, Kaduna State, Nigeria and identified at

the Herbarium unit, Department of Botany, Ahmadu Bello University, Zaria-Nigeria. The husk was washed, dried, grounded and sieved into particle size between 355 to 450  $\mu\text{m}$  size.

#### Preparation of activated carbon from castor seed shell

The castor seed shells were first carbonized using a muffle furnace set at 400  $^{\circ}\text{C}$ . This temperature was maintained for 1 hour, then left to cool to ambient temperature. The carbonized castor seed shells were then impregnated with  $\text{H}_3\text{PO}_4$  in 1:1 weight ratio and activation were then carried out using a tubular furnace set at 500  $^{\circ}\text{C}$ , which was maintained for an hour.

#### Reagents

All chemicals supplied by Merck Company, were of high analytical grade and stock solution of Congo red dye was prepared by dissolving appropriate amounts of dye in deionized water and then the desired concentrations were provided by diluting the stock solution. Stock solutions of nitric acid and NaOH 0.1N were also prepared.

#### Batch Adsorption Experiment

Design of the experiment was carried out with the aid of Design-Expert software version 10.0.3 (Stat-Ease, Inc., Minneapolis, MN 55413, USA). In this investigation, 30 batch adsorption experiments designed by central composite design (CCD) approach using RSM were conducted with ACCS as adsorbent to study the effect of initial concentrations (25-125 mg/L), dosage (0.6 - 3 g/20  $\text{cm}^3$ ), pH (2.0 - 11.0) and contact time (20 - 120 min) on the removal of Congo red dye. Samples were collected at predetermined time intervals for analyzing the residual dye concentration in the solutions and the solution volume (v) was kept constant (20  $\text{cm}^3$ ).

#### Fourier Transform Infrared (FTIR) analysis

FTIR analysis was carried out on ACCS to reveal the functional groups which aided the adsorption of Congo red dye. FTIR was used to obtain the active site on the adsorbent surface area by using the transmittance mode conducted over wavelengths of 600 – 4000  $\text{cm}^{-1}$ .

#### Modeling and statistical analysis

The experimental data were analyzed and validated for predicted response (Y). The percentage of removal is the main response which developed the model, correlating the four variables using second-degree polynomial as shown in equation below.

$$Y = b_0 + \sum_{i=1}^n b_i x_i + (\sum_{i=1}^n b_{ii} x_i)^2 + \sum_{i=1}^{n-1} \sum_{j=i+1}^n b_{ij} x_i x_j + \epsilon \quad (1)$$

Where Y is the predicted response,  $x_i$  and  $x_j$  are the input variables,  $b_0$  = Constant coefficient,  $b_i$  = Linear coefficient,  $b_{ij}$  = Interaction coefficient,  $b_{ii}$  = Quadratic coefficient and  $\epsilon$  = Random error

Coefficient of Determination ( $R^2$ ) was used to determine the quality of the model as it compared the data from predicted model with data gotten from experimental runs (Anilkumar et al., 2016). Fisher variation ratio (F-value) was employed to explain the adequacy and significance of the predicted model (Anilkumar et al., 2016).

#### Model equations for Congo red dye adsorption

The range and levels of independent process variables are summarized in Table 1. Central composite design was used to investigate the effect of four independent variables: adsorbent dose, initial concentration, pH and contact time for the removal of Congo red dye from aqueous solution using ACCS.

**Table 1: Experimental factor levels used in factorial design**

Independent variable	Factor	Coded levels				
		- $\alpha$	-1	0	+1	+ $\alpha$
Adsorbent dose (g)	A	0.6	1.2	1.8	2.5	3.0
Initial concentration (mg/L)	B	25	50	75	100	125
pH	C	2	4	6.5	9	11
Contact time (min)	D	20	45	70	95	120

#### Data Evaluation

The quality of adsorbent (q) is judged by the dye uptake (Adsorption capacity). The amount of dye bound by the adsorbent which disappeared from the solution was calculated based on the mass balance for the adsorbent in the system.

$$q = \frac{V(C_i - C_f)}{S} \quad (2)$$

q = dye uptake capacity ( $\text{mgg}^{-1}$ ),  $C_i$  = Initial concentration of dye in solution before the sorption analysis (ppm),  $C_f$  = Final concentration of dye in solution after the sorption analysis (ppm), S = weight of adsorbent (g), V = Solution volume ( $\text{cm}^3$ ).

The difference between the initial dye concentration and final dye concentration was assumed to be bound to the adsorbent. The Adsorption efficiency, A %, of the dye was calculated using equation 3.

$$A \% = \frac{C_0 - C_e}{C_0} \times 100 \quad (3)$$

Where  $C_0$  and  $C_e$  are the initial and equilibrium dye concentrations (ppm), respectively (Eletta et al., 2018).

## RESULTS AND DISCUSSION

### Characteristics of the Activated Carbon

The FTIR technique was an important tool to identify functional groups, which are capable of adsorbing Congo red dye. The measurement was done in the range of 600-4000  $\text{cm}^{-1}$ . At 1684.8  $\text{cm}^{-1}$  is a stretching mode of carbonyls mainly ketones of C=O. Intense peaks in region (1580.4 to 1423.8  $\text{cm}^{-1}$ ) originate from the secondary Amines N-H, while stretching at (1121.9  $\text{cm}^{-1}$ ) for C-O come from ethers. In the region of 1900.9  $\text{cm}^{-1}$  is a stretching mode of allene (C=C=C) while Peaks observed at (2370.6  $\text{cm}^{-1}$ ) originate from C=C or C=N. Therefore, this has confirmed that these functional groups are responsible for the adsorption by binding the dye through electrostatic or hydrogen bonding interactions.

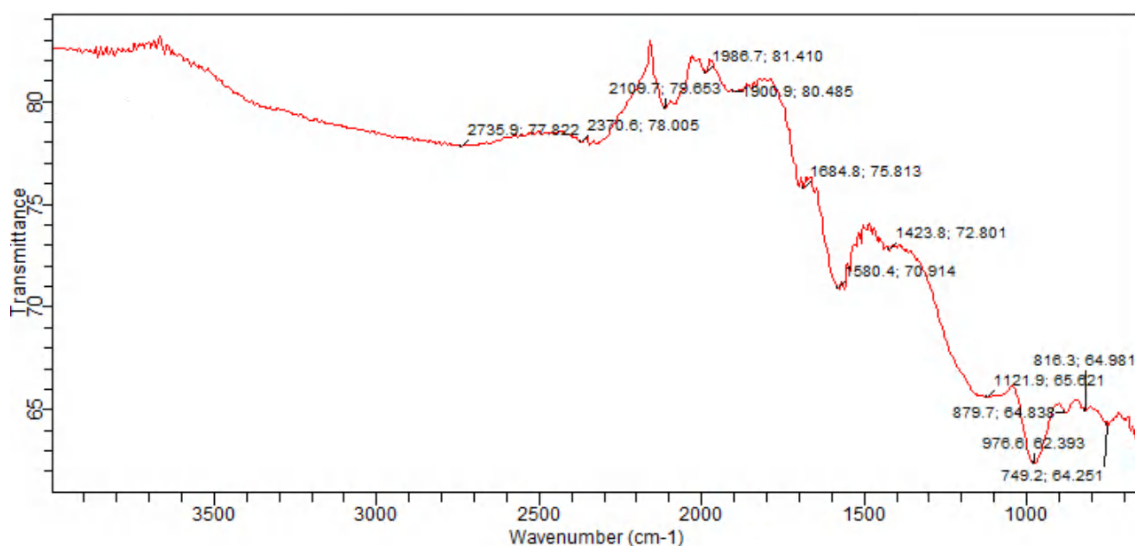


Figure 1: Fourier Transform Infrared Spectroscopy (FTIR) of ACCS

A total of 30 experiments were performed and the result of the experimental runs is presented in Table 2. At different combinations of the variables, the Congo red dye removal varied between 94.8 and 100 %.

Table 2: CCD matrix for the experimental design for Congo red dye removal using ACCS

Run	A	B	C	D	Response
1	0	- $\alpha$	- $\alpha$	0	94.8
2	- $\alpha$	-1	+1	$\alpha$	99.92
3	0	0	0	-1	99.9733
4	+1	+ $\alpha$	+ $\alpha$	+ $\alpha$	99.992
5	0	- $\alpha$	0	0	99.88
6	+ $\alpha$	-1	+ $\alpha$	+1	99.84
7	+1	- $\alpha$	- $\alpha$	- $\alpha$	99.76
8	- $\alpha$	+ $\alpha$	-1	+1	99.944
9	0	+1	0	0	99.94
10	+ $\alpha$	+1	-1	-1	99.95
11	- $\alpha$	+1	+1	+ $\alpha$	99.96
12	0	0	0	+ $\alpha$	99.9467
13	+1	+ $\alpha$	+ $\alpha$	- $\alpha$	100
14	+1	- $\alpha$	- $\alpha$	+ $\alpha$	99.68
15	-1	+1	- $\alpha$	0	99.86
16	- $\alpha$	+ $\alpha$	+ $\alpha$	- $\alpha$	99.832
17	- $\alpha$	+ $\alpha$	-1	- $\alpha$	99.888
18	-1	+1	-1	-1	99.85
19	+1	+ $\alpha$	- $\alpha$	- $\alpha$	99.784
20	0	0	- $\alpha$	-1	98.8533
21	+1	+ $\alpha$	0	-1	99.888
22	- $\alpha$	- $\alpha$	- $\alpha$	- $\alpha$	99.52
23	+1	- $\alpha$	+1	- $\alpha$	99.64
24	0	0	0	0	99.88
25	- $\alpha$	+ $\alpha$	-1	-1	99.92
26	- $\alpha$	-1	- $\alpha$	+1	99.76
27	+1	0	- $\alpha$	0	97.84
28	0	0	+ $\alpha$	- $\alpha$	99.8933

29	0	+ $\alpha$	0	0	99.936
30	- $\alpha$	+ $\alpha$	-1	0	99.936

Based on experimental data, the model (in coded form) for Congo red dye adsorption is presented in Equation 4, with positive sign of the coefficient indicating the term affecting adsorption positively while negative sign points to the adsorption being affected negatively by the term in the model equation.

$$\begin{aligned} & \% \text{ removal Congo red dye} \\ & = + 99.98 - 1.06A + 1.57C - 0.028D + 0.34AC - 0.36AD + \\ & 0.96 A^2 - 0.11B^2 - 1.00A^2D + 1.48AB^2 + 0.62 B^2D + 2.04 \\ & BC^2 - 1.83BD^2 - 1.77 CD^2 - 0.37 A^2CD - 1.42 B^2C^2 + \\ & 0.78B^2D^2 \text{ (4)} \end{aligned}$$

#### Analysis of variance (ANOVA)

Results of the significance, non-significance of the model and lack of fit respectively are displayed in Table 3, with the p-

value of the model less than 0.05 thus indicating that the model is significant. The p-value of the models lack of fit is greater than 0.05 indicating that the models lack of fit is not significant. These were further confirmed by the less than 0.2 difference between the adjusted and predicted  $R^2$ . The  $R^2$ , adjusted and predicted  $R^2$  values were found to be 0.9857, 0.9681 and 0.8236 respectively with adequate Precision of 39.572.

The value of the signal-to-noise ratio (adequate precision ratio) for the model indicated that the signal was adequate since the adequate precision ratio exceeded 4. This therefore shows that the quadratic model could be used to explore the design space and to find the optimal conditions of the adsorption process.

**Table 3: Model Significance table for Congo red dye removal using ACCS**

Source	Sum of squares	df	Mean Square	F-value	P- value	Verdict
Model	28.52	16	1.78	55.97	< 0.0001	Significant
A-dose	1.91	1	1.91	60.01	< 0.0001	
C-pH	4.47	1	4.47	140.41	< 0.0001	
D-time	2.117E-003	1	2.117E-003	0.066	0.8006	
AC	0.92	1	0.92	28.99	0.0001	
AD	0.26	1	0.26	8.18	0.0134	
A <sup>2</sup>	1.92	1	1.92	60.38	< 0.0001	
B <sup>2</sup>	0.030	1	0.030	0.95	0.3483	
A <sup>2</sup> D	0.50	1	0.50	15.54	0.0017	
AB <sup>2</sup>	1.71	1	1.71	53.55	< 0.0001	
B <sup>2</sup> D	0.38	1	0.38	11.97	0.0042	
BC <sup>2</sup>	7.59	1	7.59	238.23	< 0.0001	
BD <sup>2</sup>	6.26	1	6.26	196.65	< 0.0001	
CD <sup>2</sup>	3.72	1	3.72	116.71	< 0.0001	
A <sup>2</sup> CD	0.51	1	0.51	15.93	0.0015	
B <sup>2</sup> C <sup>2</sup>	1.81	1	1.81	56.96	< 0.0001	
B <sup>2</sup> D <sup>2</sup>	0.58	1	0.58	18.17	0.0009	
Residual	0.41	13	0.032			
Lack of fit	25.43	15	1.70	0.14	0.9969	not significant
Pure Error	36.93	3	12.31			
Cor Total	28.93	29				
R <sup>2</sup> =0.9857						
R <sup>2</sup> <sub>adj</sub> =0.9681						
R <sup>2</sup> <sub>pred.</sub> =0.8236						
Adeq Precision =39.572						

#### Optimization

The optimal values of the selected variables were obtained by solving the equation of regression in equation 4, using the

optimization module of the Design-Expert 10.0.3 (RSM) software. The first five solutions of the optimum factors predicted by the software for maximum adsorption of Congo

red dye were presented in Table 4. These were further validated by comparing experimental results to the predicted results as shown in Table 5. Strong coefficient of determination ( $R^2$ ) of 0.9997 was obtained for adsorption of Congo red dye using ACCS thus signifying less variation

between the predicted and actual values. Model predicted optimized conditions are initial concentration 100.0 mg/L, adsorption dose 1.2 g, contact time 45.0 mins and pH 4.0 giving 99.974 % removal efficiency of Congo red dye using ACCS.

**Table 4: Optimization solutions of Congo red dye removal using ACCS**

Solutions	dose*	conc*	pH*	time*	R1	Desirability	
1	<u>1.183</u>	<u>42.138</u>	<u>2.210</u>	<u>25.828</u>	<u>99.595</u>	<u>1.000</u>	<u>Selected</u>
2	0.600	50.000	11.000	120.000	99.907	1.000	
3	0.600	125.000	4.000	45.000	99.824	1.000	
4	1.200	100.000	2.000	70.000	99.798	1.000	
5	1.200	100.000	4.000	45.000	99.974	1.000	

**Table 5: Validation results of Congo red dye removal using ACCS**

Solution	% Congo red dye removal	
	Actual	Predicted
1	94.80	94.83
2	99.92	99.91
3	99.97	99.99
4	99.99	99.90
5	99.88	99.86
$R^2$	0.9997	

#### Response surface analysis for Congo red adsorption

Figures 2-6 are response surface plots. The response surface plot is a 3D graphical representation of the regression

equation. Each figure presented the effect of two variables on the removal of Congo red dye using ACCS while the other two variables were held constant at the middle level.

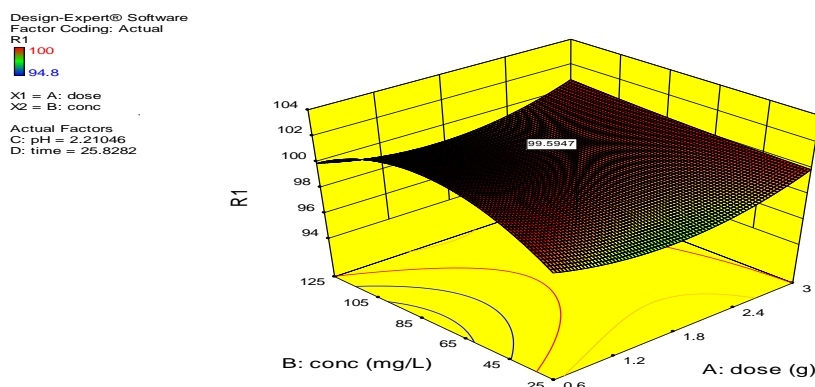


Figure 2: Effect of the interaction between adsorbent dose and initial concentration on Congo red dye removal using ACCS.

The interactive effect of adsorbent dose and initial concentration on the adsorption efficiency of Congo red dye using ACCS is shown in Figure 2. The graph shows that percentage removal of Congo red dye increased as adsorbent dose and initial concentration was increased. This is due to increase in surface area as adsorbent dose was increased (Sahu *et al.*, 2013; Postai *et al.*, 2016), and probably due to

the fact that better mass transfer occurred from aqueous medium to solid adsorbent as initial concentration was increased (Ahluwalia and Goyal, 2010). However, further increase in initial concentration from 100 to 125 mg/L led to a decrease in Congo red dye removal. This can be attributed to the fewer active sites available on the surface of ACCS as initial concentration was further increased (Eletta *et al.*, 2018)

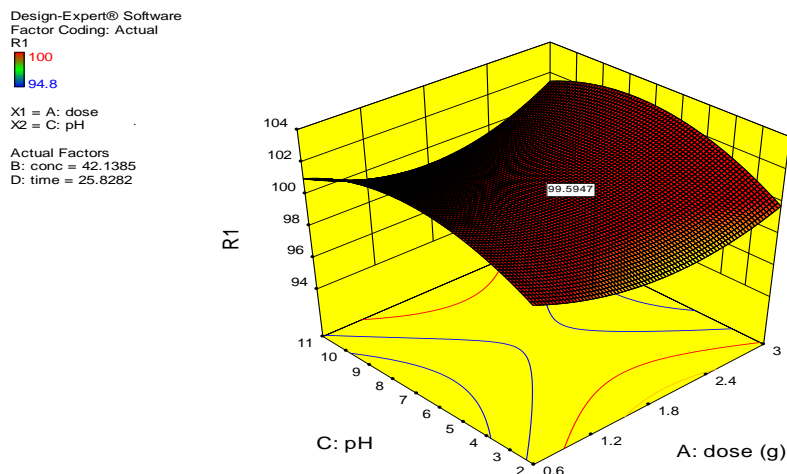


Figure 3: Effect of the interaction between adsorbent dose and pH concentration on Congo red dye removal using ACCS.

The effect of adsorbent dose and pH on the adsorption efficiency of Congo red dye using ACCS is displayed in Figure 3. It can be seen that an increase in adsorption efficiency of Congo red dye was observed with increase in pH. This may be due to the reduction in the number of hydrogen ions ( $H^+$ ) as they have faster mobility and hence get to the available active sites first (Vojnovi'c *et al.*, 2022). The interactive effect of adsorbent dose and time on the removal

efficiency of Congo red dye using ACCS is displayed in Figure 4. An increase in both adsorbent dose and contact time led to an increase in percentage removal of Congo red dye. This could be due to an increase in number of active sites available for adsorption as dose was increased (Rapo and Tonk, 2021) and due to availability of binding sites within the sorbent, since adsorption kinetics depends on the sorbent surface area (Qader and Akhtar, 2005; Vojnovi'c *et al.*, 2022).

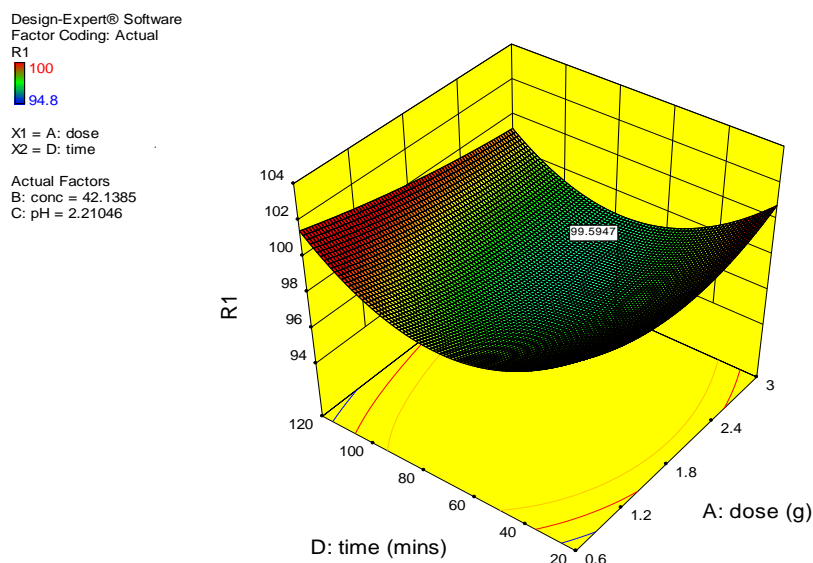


Figure 4: Effect of the interaction between adsorbent dose and contact time on Congo red dye removal using ACCS.

The interactive effect of initial concentration and pH on adsorption of Congo red dye using ACCS is displayed in Figure 5. It shows that an increase in initial concentration of Congo red dye resulted in an increase in adsorption efficiency.

This is probably due to the fact that better mass transfer occurred from aqueous medium to solid adsorbent as the initial concentration increased (Flores-Alarcon *et al.*, 2022)

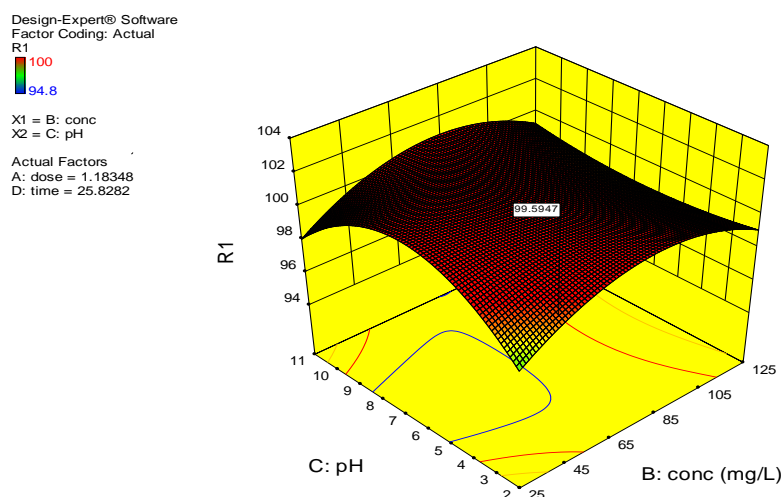


Figure 5: Effect of the interaction between pH and initial concentration on Congo red dye removal using ACCS.

However, further increase in initial concentration of Congo red dye eventually led to a decrease in percentage removal. This is due to the fact that all adsorbents have a limited number of active sites and at a certain concentration, the active sites become saturated (Vojnović *et al.*, 2022). Also, a corresponding increase in removal efficiency of Congo red dye was observed as pH was increased. This is attributed to the fact that at low pH, the functional groups available on the

adsorbents surface are highly protonated resulting in competition between the hydrogen ions and the dyes to occupy the available active sites on the adsorbent (Vojnović *et al.*, 2022). Eventually, a decrease in percentage removal was observed as pH level was further increased from pH 9. This is because at this point the hydroxide ions tend to compete with the dyes for surface area and active sites (Flores-Alarcón *et al.*, 2022)

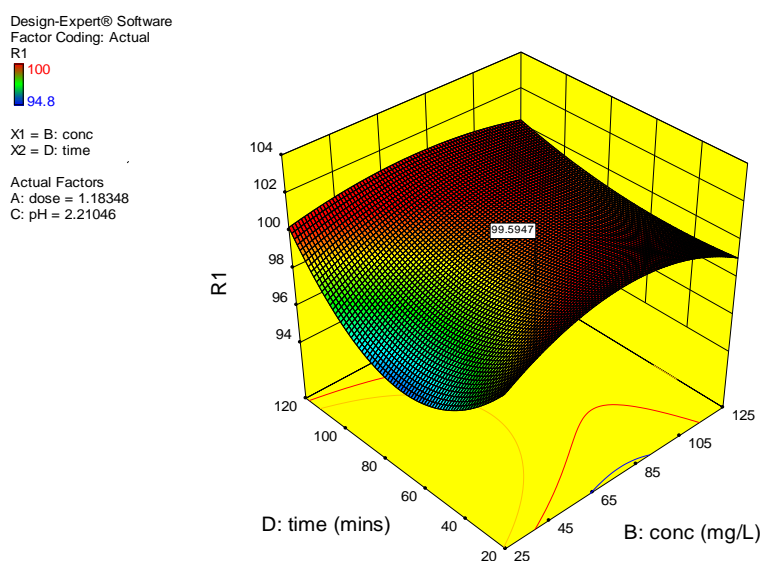


Figure 6: Effect of the interaction between contact time and initial concentration on Congo red dye removal using ACCS

Figures 6 display the effect of initial concentration and contact time on the adsorption efficiency of Congo red dye using ACCS. It shows that an increase in initial concentration of Congo red dye resulted in an increase in adsorption efficiency using ACCS. This is probably due to the fact that better mass transfer occurred from aqueous medium to solid adsorbent as initial concentration was increased (Gul *et al.*, 2022). However, further increase in initial concentration eventually led to a decrease in percentage removal. This is due

to the fact that all adsorbents have a limited number of active sites and at a certain concentration the active sites become saturated (Postai *et al.*, 2016).

An increase in removal efficiency of Congo red dye using ACCS was observed as contact time was increased. This could be due to the availability of uncovered surfaces of the adsorbent (Bayuo *et al.*, 2020). Garba *et al.* (2016) reported a research study of similar result.

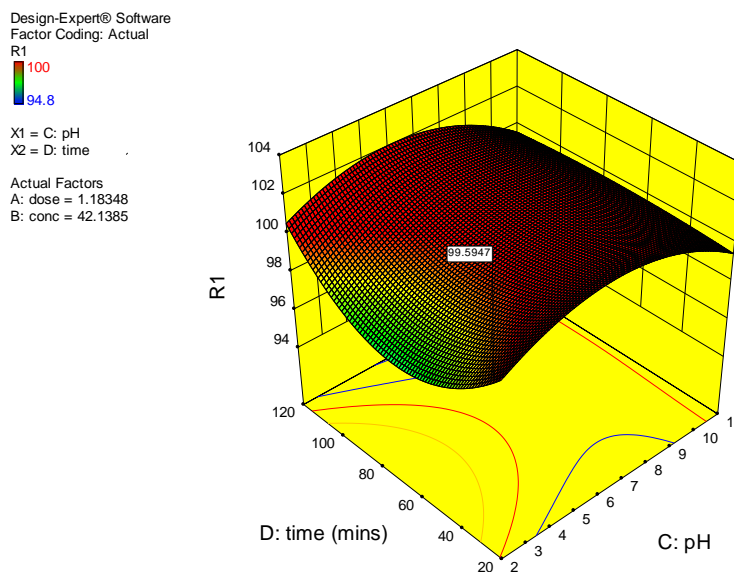


Figure 7: Effect of the interaction between contact time and pH on Congo red dye removal using ACCS

The interactive effect of pH and contact time on adsorption of Congo red dye using ACCS is displayed in Figures 7. An increase in removal efficiency of Congo red dye was observed as contact time was increased. This could be due to the availability of uncovered surfaces of the adsorbent (Bayuo *et al.*, 2020). A corresponding increase in removal efficiency of Congo red dye was observed as pH was increased. This is attributed to the fact that at low pH the functional groups available on the adsorbents surface are highly protonated resulting in competition between the hydrogen ions and the dyes to occupy the available active sites on the adsorbent (Eletta *et al.*, 2018). Eventually, a decrease in percentage removal was observed as pH level was further increased from pH 9 to pH 11. This is because at this point the hydroxide ions tend to compete with the dyes for surface area and active sites (Eletta *et al.*, 2018).

## CONCLUSION

The results obtained in this research demonstrate that activated carbon prepared from castor seed shell has high ability for adsorption of Congo red dye. The conditions for adsorption of Congo red dye were optimized and with advantage of high dye adsorption capacity. Conclusively, activated carbon produced from castor seed shell can be used as an efficient and economic adsorbent material for the removal of Congo red dye from aqueous solution.

## REFERENCES

Adetokun, A. A., Uba, S., Garba, Z. N. (2019). Optimization of adsorption of metal ions from a ternary aqueous solution with activated carbon from *Acacia senegal* (L.) Willd pods using Central Composite Design. *Journal of King Saud University - Science*, Article in Press, <https://doi.org/10.1016/j.jksus.2018.12.007>.

Afidah, A. R., Garba, Z.N. (2016). Efficient adsorption of 4-Chloroguaiacol from aqueous solution using optimal activated carbon: Equilibrium isotherms and kinetics modeling. *Journal Association Arab Universities Basic Applied Science*, 21, 17-23.

Akpomie, K.G. Dawodu, F.A. and Adebowale, K.O. (2015). Mechanism on the sorption of heavy metals from binary

solution by a low-cost montmorillonite and its desorption potential. *Alexandria Engineering Journal*, 54: 757–767.

Alsas, S. A., Zaharaddeen, N. G. and Sallau, M. S. (2022). Nickel adsorption onto sweet dattock shell: statistical error function models as parametric isotherm predictors. *FUDMA Journal of Sciences (FJS)*, 6 (2): 208 – 220. ISSN online: 2616-1370 ISSN print: 2645 - 2944 DOI: <https://doi.org/10.33003/fjs-2022-0602-962>

Anilkumar, B., Chitti, N. B. and Kavitha, G. (2016). Biosorption of Zinc on to *Gracilaria corticata* (Red Algae) Powder and Optimization using Central Composite Design. *Journal Applied Science and Engineering Methodologies*, 2 (3): 412–425.

Bayuo, J.; Abukari M. A. and Pelig-Ba, K. B. (2020). Optimization using central composite design (CCD) of response surface methodology (RSM) for biosorption of hexavalent chromium from aqueous media. *Applied Water Science* 10:1-12. <https://doi.org/10.1007/s13201-020-01213-3>

Eletta, O. A. A., Mustapha, S. I., Ajayi, O. A. and Ahmed, A. T. (2018). Optimization of Dye Removal from Textile Wastewater using Activated Carbon from Sawdust. *Nigerian Journal of Technological Development*, 15 (1): 26 – 32. doi: <http://dx.doi.org/10.4314/njtd.v15i1.5>

Ferreira, L. M., de-Melo, R. F., Pimeta, A. S., de-Azevedo, T. K. B. and de-Souza, C. B. (2020). Adsorption performance of activated charcoal from castor seed cake prepared by chemical activation with phosphoric acid. *Biomass Conversion and Biorefinery*, 2:1-12. <https://doi.org/10.1007/s13399-020-00660-x>

Flores-Alarcón, M. A. D., Revilla-Pacheco, C., Garcia-Bustos, K., Tejada-Meza, K., Terán-Hilares, F., Pacheco-Tanaka, D. A., Colina-Andrade, G. J. and Terán-Hilares, R. (2022). Efficient dye removal from real textile wastewater using orange seed powder as suitable bio-adsorbent and membrane technology. *Water*, 4104: 1-14. <https://doi.org/10.3390/w14244104>

- Garba, Z. N., Bello, I., Galadima, A. and Lawal, A. Y. (2015). Optimization of adsorption conditions using central composite design for the removal of copper (II) and lead (II) by defatted papaya seed. *Karbala International Journal of Modern Science* xx (2015): 1-9. <http://dx.doi.org/10.1016/j.kijoms.2015.12.002>. Available online at [www.sciencedirect.com](http://www.sciencedirect.com)
- Garba, Z. N., Zango, Z. U., Babando, A. A. and Galadima, A. (2016). Competitive adsorption of dyes onto granular activated carbon. *Journal of Chemical and Pharmaceutical Research*, 7(4):710-717.
- Garba, Z. N., Abdullahi, A.K., Haruna, A., Gana, S.A. (2021). Risk assessment and the adsorptive removal of some pesticides from synthetic wastewater: a review. *Beni-Suef Univ. J. Basic Appl. Sci.*, 10, <https://doi.org/10.1186/s43088-021-00109-8>.
- Gul, S., Gul, H., Gul, M., Khattak, R., Rukh, G., Khan, M. S. and Aouissi, H. A. (2022). Enhanced adsorption of rhodamine B on biomass of Cypress/False Cypress (*Chamaecyparis lawsoniana*) Fruit: optimization and kinetic study. *Water*, 2987: 1-12. <https://doi.org/10.3390/w14192987>
- Kooh, M. R. R., Dahri, M.K. and Lim, L.B. (2016). The removal of rhodamine B dye from aqueous solution using *Casuarina equisetifolia* needles as adsorbent. *Cogent Environmental Science*, 2: 1-10.
- Labaran, A.N., Zango, Z.U., Armayau, U., Garba, Z. N. (2019). Rice husk as biosorbent for the adsorption of methylene blue. *Science World Journal*, 14: 66-69.
- Lofrano, G., Brown, J. and Feo, G. D. (2012). Green practices to save our precious “water resource”. In Sharma K. S. and Shangai R. (Ed.), *Advances in Water Treatment and Pollution Prevention* (37). Dordrecht: *Springer Science Business Media*. Doi:10.1007/978-94-007-4204-8\_5
- Malik, A., Khan, A., Anwar, N. and Naeem, M. (2020). A comparative study of the adsorption of Congo Red Dye on rice husk, rice husk char and chemically modified rice husk char from aqueous media. *Bull. Chemical Society of Ethiopia*, 34(1): 41-54. Downloaded on 07/03/2023 from <https://dx.doi.org/10.4314/bcse.v34i1.4>
- Postai, D. L., Demarchi, C. A., Zanatta, F., Melo, D. C. C. and Rodrigues, C. A. (2016). Adsorption of rhodamine B and methylene blue dyes using waste of seeds of *Aleurites Moluccana*, a low-cost adsorbent. *Alexandria Engineering Journal*, 55: 1713–1723.
- Rápo, E. and Tonk, S. (2021). Factors affecting synthetic dye adsorption; desorption studies: a review of results from the last five years (2017–2021). *Molecules*, 26: 5419. <https://doi.org/10.3390/molecules26175419>. Available online at <https://www.mdpi.com/journal/molecules>.
- Surip, S.N., Abdulhameed, A.S., Garba, Z.N., Syed-Hassan, S.A., Ismail, K., Jawad, A.H. (2020). H<sub>2</sub>SO<sub>4</sub>-treated Malaysian low rank coal for methylene blue dye decolourization and cod reduction: Optimization of adsorption and mechanism study. *Surface Interface*, 21:100641.
- Tan, C. H. C., Sabar, S., Haafiz, M.K.M., Garba, Z. N., Hussin, M. H. (2020). The improved adsorbent properties of microcrystalline cellulose from oil palm fronds through immobilization technique. *Surface Interface*, 20: 100641.
- Vojnović, B., Cetina, M., Franjković, P. and Sutlović, A. (2022). Influence of initial pH value on the adsorption of reactive black 5 dye on powdered activated carbon: Kinetics, Mechanisms, and Thermodynamics. *Molecules*, 1349: 1-12. <https://doi.org/10.3390/molecules27041349>
- Xiao, W., Garba, Z. N., Sun, S., Lawan, I., Wang, L., Lin, M., Yuan, Z. (2020). Preparation and evaluation of an effective activated carbon from white sugar for the adsorption of rhodamine B dye. *Journal Clean-water Production*, 253: 119989.
- Xiao, W., Jiang, X., Liu, X., Zhou, W., Garba, Z. N., Lawan, I., Wang, L., Yuan, Z. (2021). Adsorption of organic dyes from wastewater by metal-doped porous carbon materials. *Journal of Clean. Production*, 284: 124773

